ELSEVIER

Journal of Magnetism and Magnetic Materials 210 (2000) 316–328

Journal of magnetism and magnetic materials

www.elsevier.com/locate/jmmm

The influence of CO and H_2 adsorption on the spin reorientation transition in Ni/Cu(0 0 1)

S. van Dijken[a,*], R. Vollmer[b], B. Poelsema[a], J. Kirschner[b]

[a]*Faculty of Applied Physics and MESA + Research Institute, University of Twente, P.O. Box 217, NL-7500 AE Enschede, The Netherlands*
[b]*Max-Planck-Institut für Mikrostrukturphysik, Weinberg 2, D-06120 Halle/Saale Germany*

Received 28 July 1999

Abstract

A strong reduction of the critical thickness of the spin reorientation transition in Ni/Cu(0 0 1) has been observed when covered with CO or H_2. For uncovered Ni films a critical thickness of 10.5 ML has been found at $T = 300$ K. The critical thickness is reduced by about 3 and 4 ML after adsorption of 0.5 ML CO and H_2, respectively. The observed shift in the spin reorientation transition implies a reduction of the negative surface anisotropy energy by about 50% in both cases.

PACS: 75.70.Ak; 78.20.Ls; 68.55. − a

Keywords: Thin films; Spin reorientation transition; Surface anisotropy; Kerr microscopy

1. Introduction

Ultrathin ferromagnetic layers often show a different magnetic behavior than the bulk. Reduced symmetry and a modified lattice constant for a pseudomorphic growth may change the magnetic moment and influence the direction of the magnetization axis. The direction of the magnetization in the remanent state is determined within the phenomenological model by the interplay of a thickness-dependent part (surface/interface anisotropy) and a thickness-independent part (volume anisotropy) of the magnetocrystalline anisotropy energy density and the shape (or more precise the dipolar) anisotropy energy density. A spin reorientation transition may occur when these three anisotropies do not have the same signs. Reorientation from out-of-plane to in-plane magnetization has been observed for a number of ultrathin magnetic films, typically in the 2–6 monolayer (ML) thickness range [1–3]. Contrary to this, a transition from in-plane magnetization to out-plane magnetization at 7–10 ML has been measured for Ni films on Cu(0 0 1) [4–8]. The in-plane magnetization is caused by a large thickness-dependent negative surface and interface anisotropy. Therefore, a change in surface or interface anisotropy will shift the spin reorientation transition to a different Ni film thickness. Possible ways to influence the surface anisotropy are growth of a metallic overlayer, variation of the surface roughness or adsorption of a gas. For

* Corresponding author. Tel.: + 31-534-893-148; fax: + 31-534-891-101.
E-mail address: s.vandijken@tn.utwente.nl (S. van Dijken)

0304-8853/00/$ - see front matter
PII: S0304-8853(99)00622-8

Ni on Cu(0 0 1) the effect of overlayers [9–13] and surface roughness [14] have been studied recently, while less attention has been paid to the influence of gaseous adsorbates. However, changes in the magnetic moment of the first layer have been found after hydrogen adsorption on Ni(1 1 1) [15] and Ni(0 0 1) [16–18] in the past. It is therefore expected that gaseous adsorbates will influence the spin reorientation transition in thin Ni films on Cu(0 0 1) as well.

In this paper, we will present experimental results on the effects of CO and H_2 adsorption on Ni/Cu(0 0 1). Thereafter, these results will be compared to the measured influence of a Cu cap layer and surface roughness. The paper is organized as follows. In Section 2, we present the currently generally accepted phenomenological model for the magnetic anisotropy energies in Ni/Cu(0 0 1). In Section 3, a summary of the adsorption/desorption kinetics of CO and H_2 on Ni(0 0 1) is given. Section 4, describes the experimental details. In Section 5 the experimental data are presented and the results are discussed. Section 6 summarizes this work.

2. Spin reorientation transition

The anomalous spin reorientation transition of Ni films on Cu(0 0 1) has intensively been investigated during the last years [4–14,19–24]. The spin reorientation transition is described by an effective second order magnetization anisotropy energy (per unit cell volume) K_2 and a shape anisotropy energy $2\pi M_s^2$ (M_s is the saturation magnetization). K_2 is written, for small film thickness, as the sum of the thickness independent volume anisotropy (K_{2v}) and the thickness dependent surface (K_{2s}) and interface anisotropy (K_{2i}). Perpendicular magnetization will result when $K_{2v} + (K_{2s} + K_{2i})/d > 2\pi M_s^2$ in the Ni film. Normally, K_{2v} describes the magnetocrystalline bulk anisotropy. However, the growth of Ni on Cu(0 0 1) is pseudomorphic up to a film thickness of at least 11 ML [11,25]. In comparison with bulk FCC Ni ($\alpha_p = 2.49$ Å) the tetragonally distorted (FCT) lattice is expanded by 2.5% in the film plane and compressed by 3.2% along the surface normal [25]. The tetragonal distortion leads to an additional uniaxial anisotropy energy term absent in bulk Ni. In the literature, this term has been discussed in terms of (bulk) magnetoelastic energy [10,12,26] with [12,26] or without [10] inclusion of a surface magnetoelastic contribution. In this paper, we do not make use of these models but use a simpler and less ambiguous description of only a surface and interface part of the magnetocrystalline anisotropy, K_{2s} and K_{2i}, respectively, describing the volume dependent part of the anisotropy energy per unit cell and a volume anisotropy K_{2v}, which is a function of the magnitude of the tetragonal distortion of the Ni film: $K_2 = K_{2v} + (K_{2s} + K_{2i})/d$. The (higher order) magnetocrystalline anisotropy of bulk Ni can be ignored completely because it is about two orders of magnitude smaller (≈ -0.39 μeV/atom) than the strain induced component $K_{2v} = 30$ μeV/atom [4].

For thin Ni films on Cu(0 0 1) the positive volume anisotropy is compensated by large negative surface and interface anisotropies. Therefore, contrary to most magnetic systems, the magnetization of thin Ni films is in-plane up to a critical thickness d_c, where K_2 equals the shape anisotropy $2\pi M_s^2$ and the magnetization switches to out-plane. In literature, critical thickness values ranging from 7 ML [4–6], 8 ML [7] up to 10 ML [8] have been reported. The stress in the Ni film, which is induced by the tetragonal distortion, increases with increasing film thickness. This continues up to a critical thickness ($\geqslant 11$ ML), where the onset of strain relaxation reduces the tetragonal distortion. From there on, the volume anisotropy K_{2v} becomes thickness dependent and decreases with reduced lattice distortion, i.e. with increasing film thickness. Consequently, a second spin reorientation occurs at a thickness d_{2c}, where the effective second-order magnetocrystalline anisotropy energy K_2 equals the shape anisotropy $2\pi M_s^2$. This spin reorientation transition is less sharp than the first one, occurring at a thickness of 37 ML [10] to 50 ML [11].

3. CO and H_2 adsorption

In the past, in depth studies have been made on the adsorption/desorption kinetics and corresponding structure of CO and H_2 on Ni(0 0 1).

In this section, a summary of the relevant results is given. The CO molecules adsorb on top of Ni surface atoms for coverages up to 0.5 ML [27–32]. The orientation of the CO molecule at such a terminal adsorption site is perpendicular to the surface with the carbon bonded to a Ni surface atom [33,34]. Low-energy electron diffraction measurements always show a clear $c(2\times 2)$ superstructure for coverages up to 0.5 ML [33–36]. For temperatures below 160 K the complete $c(2\times 2)$ structure is developed at an exposure of about 2 ML [27,36]. For a coverage between 0.25 and 0.5 ML a partial occupation of bridge sites has been reported by some authors [28,32] while others found only top site adsorption up to 0.5 ML CO coverage [31]. Upon further CO exposure two new patterns develop. First, a transition to a $c(5\sqrt{2}\times\sqrt{2})R45^\circ$ superstructure with a coverage of 0.6 ML occurs which is followed by a transition to a $p(3\sqrt{2}\times\sqrt{2})R45^\circ$ structure with a coverage of 0.68 ML (saturation coverage for $T<250$ K) [31,37]. Thermal desorption spectra for CO adsorbed in the $c(2\times 2)$ structure on Ni(0 0 1) show a peak labeled β_2 at about 440 K for heating rates of about 10–15 K/s [28,32,38,39]. The isosteric heat of adsorption in this state is about 1.25 eV/CO molecule [36,38]. For coverages between 0.25 and 0.5 ML a shoulder at 350 K (labeled β_1) develops. The thermal desorption spectra for CO adsorbed in the more dense $p(3\sqrt{2}\times\sqrt{2})R45^\circ$ structure show an additional peak at about 280 K.

The adsorption/desorption behavior and structure of H_2 on Ni(0 0 1) is less complex than that of CO. H_2 adsorbs dissociatively on Ni(0 0 1) in fourfold hollow sites [40,41]. No ordered surface structure forms at a substrate temperature of 300 K [42,43]. At 200 K a quasi-ordered $p(2\times 2)$ overlayer structure develops after adsorption of 0.5 L H_2 (which corresponds to a coverage of about 0.5 ML of H atoms) [40]. For low and medium hydrogen exposures (up to 5 L at 100 K) the thermal desorption spectra consist of only one peak, labeled β_2, at about 350 K for a heating rate of about 15 K/s [38,39,43]. Upon further exposure (exposure >10 L H_2) a shoulder develops (β_1), which population is much less than those of the main desorption state. The isosteric heat of adsorption in the β_2 state is about 1.0 eV/H_2 molecule [43,44].

4. Experimental

Our experiments were conducted in ultra-high vacuum (base pressure $<4\times10^{-11}$ mbar) using Kerr microscopy, low- and medium-energy electron diffraction (LEED/MEED) and Auger electron spectroscopy (AES). The sample was cut from a single-crystal Cu rod, oriented with the aid of an X-ray diffractometer and mechanically and electrochemically polished, resulting in a miscut less than 0.2°. The sample was heated in an Ar/H_2 atmosphere at about 820 K for several hours. After insertion into the UHV chamber the sample was cleaned by a few cycles of sputtering with 2 keV Ar^+ ions and prolonged heating at 840 K. This procedure resulted in a clean and well-ordered surface as was determined by AES and LEED. Wedge-like Ni films were grown with electron-beam evaporation on a Cu(0 0 1) surface at a temperature of 298 K. The growth rate, calibrated with MEED before growth of the wedge and checked by AES after Kerr microscopy measurements, was about 0.5 ML/min. During growth the pressure in the vacuum chamber never exceeded 2×10^{-10} mbar. In-situ Kerr microscopy measurements were performed using a similar setup as described in Ref. [45]. The microscope, shown in Fig. 1, has two separate sections; an illumination part and a subsystem with a long distance microscope objective mounted to a CCD camera. The illumination section is attached to one of the vacuum chamber

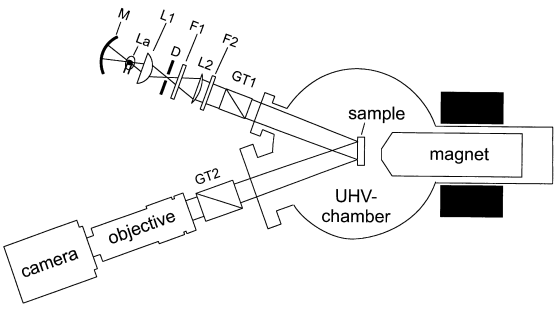

Fig. 1. Schematic view of the experimental Kerr microscopy setup: M: mirror, La: halogen lamp, L1: condensor, D: diaphragm, F1, F2 infrared and blue blocking filters, L2: lens $f=100$ mm, GT1: Glan–Thompson polarizer, GT2: analyzer (Glan–Thompson), O: long distance objective, C: CCD camera.

windows and consists of a 50 W halogen lamp, collimating optics, blue and infrared blocking filters, a focusing lens, and a Glan–Thompson polarizer. Another vacuum chamber port is used for the microscope objective and the CCD camera. In front of the microscope objective a second Glan–Thompson is placed for polarization analysis. The sample is illuminated with an incident angle of 20° with respect to the surface normal. Kerr microscopy measurements were performed in the polar geometry i.e., with the external magnetic field oriented normal to the surface. Images were taken with the repeated sequence of -300, 0, $+300$, 0 Oe external field at an acquisition time of about 10 s/image. From each sequence two asymmetry images, i.e. the difference of two images divided by their sum, were constructed: one for the remanent state and one for an external magnetic field of 300 Oe. With this setup it was possible to measure the change in the critical thickness of the spin reorientation transition *during* the adsorption of CO and H_2. In the adsorption experiments the wedge like Ni film was exposed to the adsorbate at $T = 143$ K and a pressure of 1×10^{-9} mbar. In order to exclude surface roughness induced changes in the spin reorientation transition, the Ni film was annealed to 453 K prior to adsorbate adsorption. This results in a smooth Ni surface without any significant substrate interdiffusion [23,46]. In addition to the Kerr images measurements of full hysteresis curves were performed using a standard polar Kerr setup with a laser diode ($\lambda = 670$ nm) as light source and a photodiode as detector.

5. Results

5.1. CO/Ni/Cu(0 0 1)

On the Cu(0 0 1) surface a Ni wedge, ranging from 3.9 to 12.5 ML, was grown to study CO adsorption. The changes in the spin reorientation transition during CO adsorption, as monitored by Kerr microscopy imaging, is displayed in Fig. 2. This figure shows selected stripes of remanent state asymmetry images for five CO exposures at $T = 143$ K. The imaged surface area is the same for each stripe and corresponds to 0.6 mm × 5 mm. For the clean Ni film (first stripe), up to a film thickness of about 11 ML no Kerr asymmetry is measured, i.e. the magnetization is in-plane. However, at 11 ML a very fast increase in the polar Kerr signal is observed, followed by a linear increase in the remanent asymmetry with film thickness. The spin reorientation in the remanent state occurs within a thickness range of one monolayer. The thickness d_c at which the spin reorientation from in-plane magnetization to perpendicular magnetization occurs, is not related to the thickness at which a dislocation network starts to develop to reduce film strain. O'Brien et al. [11] found a strong increase in the coercive field at a thickness of 13 ML, which can be interpreted as the onset of dislocation formation. This is in agreement with our own Kerr measurements shown in Fig. 3 where we observe this strong increase of the coercive field at about 16 ML. Furthermore, Müller et al. [25] found no significant reduction of the tetragonal distortion up to a film thickness of at least 11 ML. The spin reorientation transition of the clean Ni film is therefore below this onset of misfit dislocations. Exposure to CO immediately shifts the border of the spin reorientation transition to smaller film thickness.

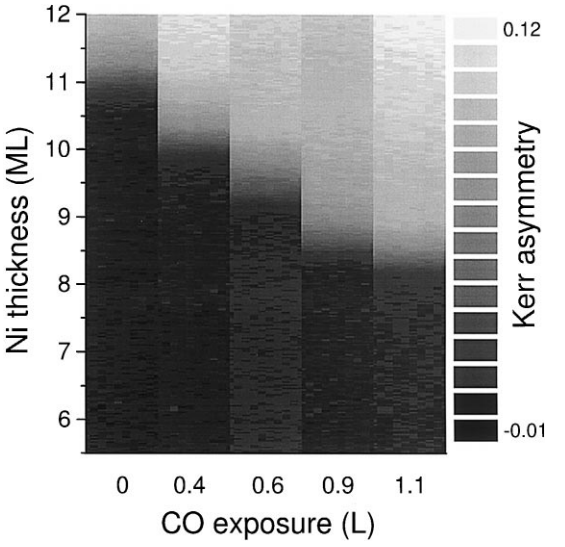

Fig. 2. Polar remanent Kerr asymmetry images of the same section of a Ni wedge on Cu(0 0 1) for five CO exposures at 143 K.

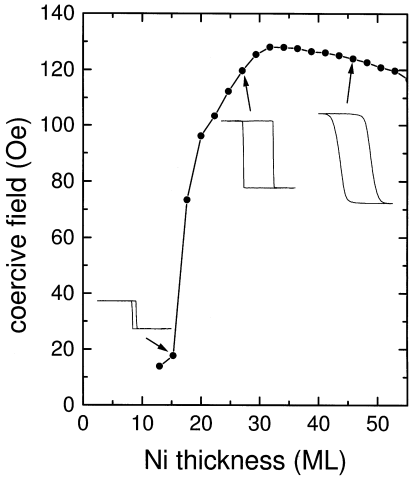

Fig. 3. Coercive field versus Ni film thickness. A strong increase in the coercive field is observed at 16 ML.

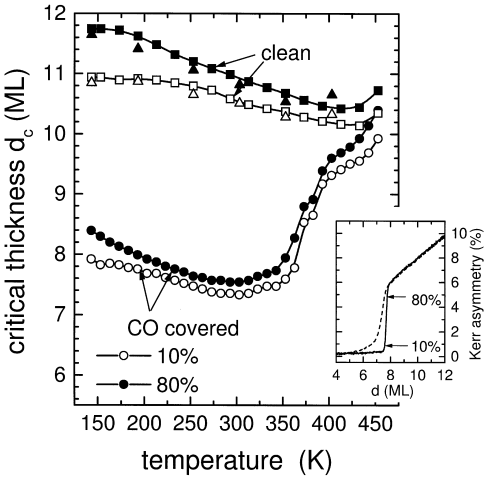

Fig. 4. Critical thickness of the spin reorientation transition of a Ni film versus sample temperature for the clean surface (squares), for the surface exposed to 1.2 L CO at 143 K (circles) and for the CO covered surface after annealing at 453 K (triangles). Open (closed) symbols represent the thickness at which the remanent Kerr signal is dropped to 10% (80%) of the extrapolated polar Kerr signal of the same thickness. The increase of the critical thickness at about 320 K is caused by the onset of CO desorption. The inset shows the measured Kerr asymmetry as a function of the Ni thickness at 233 K for the CO covered film.

The exposure is determined from the pressure as read from the ion gauge without any further corrections. The actual CO exposure is somewhat larger (by a factor 2 maximum) due to the position of the ion gauge with respect to substrate and gas inlet. The critical thickness is decreased down to 8 ML after a CO exposure of only 1.1 L. No further shift of the spin reorientation transition to smaller film thicknesses is measured upon further exposure. Compared to CO adsorption measurements in Refs. [27,36], the actual CO coverage at which the shift in spin reorientation saturates is close to 0.5 ML, with the CO molecules adsorbed in a $c(2\times 2)$ overlayer structure.

Fig. 4 shows the critical thickness d_c as a function of sample temperature for the clean (squares) and CO covered surface (circles and triangles for increasing and decreasing temperature, respectively). The average measured time per data point for the CO covered surface was about 5 min, which corresponds to a heating/cooling rate of 0.03 K/s. In order to avoid gas adsorption at low temperatures on the clean surface, the data points for this surface were taken with decreasing sample temperature. Open (closed) symbols indicate the thickness at which the remanent Kerr signal dropped to 10% (80%) of the extrapolated polar Kerr signal of the same thickness. The inset shows the remanent Kerr signal as a function of film thickness for the CO covered surface at $T = 233$ K. At this temperature the reorientation from in-plane to perpendicular remanent magnetization occurs in a small thickness range of less than 0.2 ML. The measured critical thickness d_c for the CO covered surface (increasing sample temperature) decreases linearly to 7.4 ML at $T = 300$ K. At about 320 K the border of the spin reorientation transition starts to increase. This increase can be attributed completely to the onset of CO desorption from the Ni surface. As mentioned in Section 3 TPD measurements show a CO desorption peak at about 440 K [28,32,38,39] (β_2 desorption peak) for a heating rate of about 15 K/s. Because of our much lower heating rate of only 0.03 K/s the peak desorption occurs at lower temperatures: the strong increase of the critical thickness at about 380 K is in complete agreement with the TPD measurements indicating a desorption energy of about 1.25 eV (first-order desorption kinetics and a pre-exponential factor of 2×10^{14} is assumed). The weak increase of d_c at lower

temperatures below 380 K might be due to desorption from the slightly weaker bound β_1 adsorption site. At a sample temperature of 453 K the critical thickness of the CO covered surface is almost equal to the one measured for the clean Ni film. Annealing at this temperature for several minutes results in a critical thickness (10.4 ML (10% data points)), which is equal to the clean Ni film. From this we conclude that 453 K is sufficient to clean the surface. Auger electron spectroscopy confirms this; only a small fraction of CO (close to the detection limit of the CMA Auger spectrometer) remained on the Ni surface, which does not change the thickness of the spin reorientation transition significantly. This is illustrated by the data points for decreasing temperature. The critical thickness for the CO covered and annealed film (triangles) and the clean film (squares) is the same within the experimental error in the whole temperature range measured.

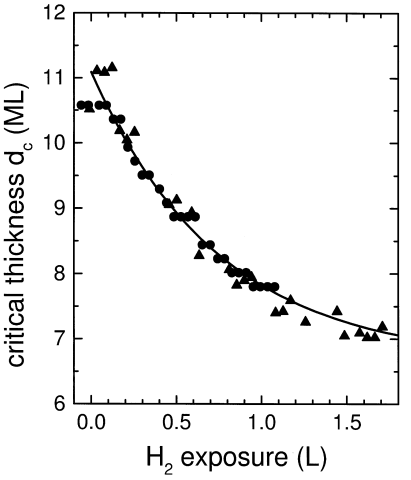

Fig. 5. Critical thickness of the spin reorientation transition of a Ni film versus hydrogen exposure at 143 K. The circular and triangular data points were measured on two different Ni wedges. An exponentially decaying fit function to the data points is shown as a solid line.

5.2. H_2/Ni/Cu(0 0 1)

As we have shown earlier [47], adsorption of hydrogen drastically influences the spin reorientation in Ni films on Cu(0 0 1). An approximate hydrogen exposure of 4 L at 143 K reduces the critical thickness by about 4 ML. Exposing more H_2 to the surface does not change the spin reorientation transition any further. Comparing with hydrogen adsorption measurements in Refs. [40,43], the actual hydrogen coverage at which the shift in spin reorientation saturates is close to 1 ML H atom coverage. From Kerr images taken during the H_2 exposure of the Ni wedge at 143 K we determined the critical thickness (taken as the thickness where the Kerr signal with a 300 Oe external field dropped to $\frac{1}{2}$ of the extrapolated full polar signal). The result from two different Ni wedges are shown in Fig. 5 versus the H_2 exposure. The displayed exposure, measured with an ion gauge, is not corrected for the hydrogen ionization probability, the position of the gas inlet and the ion gauge with respect to the substrate. The actual H_2 exposure is 3–4 times larger. Christmann et al. [43] showed that adsorption of hydrogen on Ni(0 0 1) obeys a first-order adsorption process. This implies a linear decrease of the sticking coefficient with increasing coverage. Neglecting desorption this will result in a time dependence of the hydrogen coverage $\theta(t)$ proportional to $1 - \exp(-ct)$, with c being a constant and t the exposure time. In our experiments, in which hydrogen is adsorbed at 143 K, hydrogen desorption can be neglected. As can be seen in Fig. 5, the measured critical thickness decays exponentially with hydrogen exposure as well. An exponentially decaying fit function to the data points is shown as a solid line. This leads us to conclude that the hydrogen coverage and the critical thickness have the same hydrogen exposure dependence, suggesting that the critical thickness decreases linearly with hydrogen coverage.

The temperature dependence of the critical thickness for H_2 covered Ni films is illustrated in Fig. 6. The border of the spin reorientation transition hardly changes upon heating up to about 270 K. At this substrate temperature however, a shift to larger film thickness is observed. This shift is entirely attributed to the onset of hydrogen desorption. Analogous to the case of CO adsorption discussed above the maximum hydrogen desorption occurs at about 300 K in our case which is lower than that observed in usual TPD spectra [38,39] because of the much lower heating rate (about 0.03 K/s in our case compared to 15 K/s in Ref. [39]). Assuming

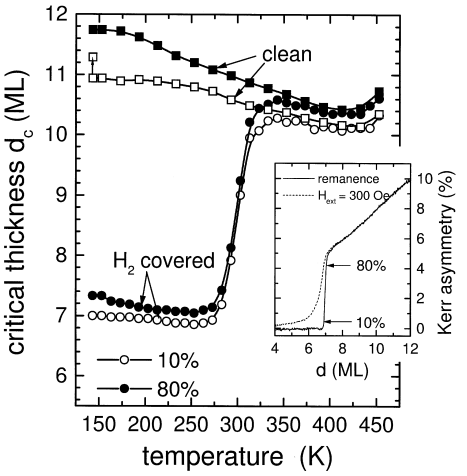

Fig. 6. Critical thickness of the spin reorientation transition of a Ni film versus sample temperature for the clean surface (squares) and for the surface exposed to 1.5 L hydrogen at 143 K (circles). Open (closed) symbols represents the thickness at which the remanent Kerr signal is dropped to 10% (80%) of the extrapolated polar Kerr signal of the same thickness. The increase of the critical thickness at about 270 K is caused by the onset of hydrogen desorption. The inset shows the measured Kerr asymmetry as a function of the Ni thickness at 233 K for the hydrogen covered film. The small arrow at the open squares at $T = 143$ K indicates an estimate of the reduction of the critical thickness by possibly adsorbed small traces of hydrogen at low temperature.

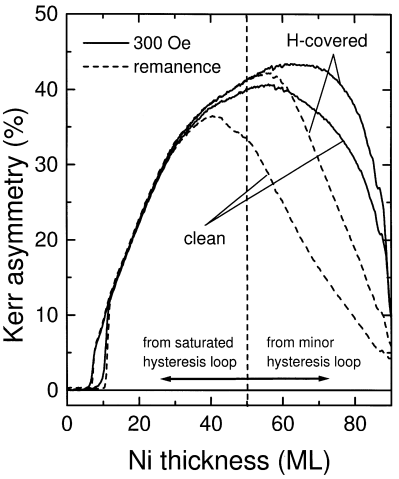

Fig. 7. Polar Kerr asymmetry versus Ni film thickness in the remanent state (dashed line) and in the magnetization state with an applied external field of 300 Oe (solid line) for a hydrogen covered and clean Ni film at 273 K.

second-order desorption kinetics the shift of 50 K of the desorption peak is consistent with a desorption energy of 1.0 eV/H_2 molecule if we assume a pre-exponential factor of about 10^{15}. The temperature interval at which the desorption occurs in Fig. 6 is narrower than in the case of the CO shown in Fig. 4 in agreement with the less pronounced β_1 TPD peak in the case of hydrogen desorption. At a substrate temperature of 330 K the critical thickness merges into the curves for the clean Ni film within experimental error. The close similarity of the behavior of (the derivative of) the critical thickness d_c and the TPD spectra gives an additional indication of the linear dependence of d_c and the hydrogen coverage. Therefore, this change of d_c can be attributed entirely to a change in the surface anisotropy constant K_{2s}.

From a change of K_{2s} upon hydrogen exposure, a shift not only in the first spin reorientation transition is expected but a change of the critical thickness in the second spin reorientation transition is expected as well. To investigate the influence of hydrogen adsorption on the second critical thickness d_{2c} we grew a Ni wedge ranging from 0 to 90 ML. In Fig. 7 the polar Kerr signal as a function of the Ni thickness at $T = 273$ K is derived from Kerr images of this steep Ni wedge for the clean and hydrogen covered film. The solid lines represent the Kerr signal with applied external field of 300 Oe and the dashed lines the remanent Kerr signal. Because of our limited external magnetic field saturation of the Ni film could be achieved only for Ni films below a thickness of about 50 ML. The Kerr asymmetry for larger Ni thickness represents the corresponding quantities from a minor hysteresis loop with an field amplitude of 300 Oe. Therefore, a reduction of the Kerr signal does not necessarily mean a reduction of the Kerr signal in the magnetically saturated state. Nevertheless, we observe in the whole thickness range, starting from the first spin reorientation transition up to more than 80 ML always a nonvanishing polar Kerr signal, both in the remanent as well as with 300 Oe applied external field, indicating that the second spin reorientation occurs over a broad thickness range. This behavior is in qualitative agreement with the measurements of Ref. [11], which also

showed a gradual transition to in-plane magnetization, over a thickness range of about 15 ML. The onset of an in-plane signal and the onset of the reduction of the remanent polar XMCD-signal was found at about 40 ML. Bochi et al. [26] and Jungblut et al. [10] found an already entirely in-plane magnetization for Ni films thicker than 60 ML. In our case, the transition range seems to be somewhat wider, which might originate in different preparation methods of the films affecting the strain relaxation. In our case, up to about 50 ML both the clean and the hydrogen covered film show perpendicular magnetization. The measurements at 300 Oe for thicker films cannot be used, because a change in this signal may simply be caused by a change of the coercivity and therefore difficult to interpret.

While for thin Ni films remanent Kerr signal and the Kerr signal at saturation coincide indicating rectangular hysteresis loops, for the clean Ni film the remanent Kerr signal starts to deviate from the saturation value at about 45 ML. For this thickness the external field of 300 Oe is still sufficient to saturate the film as can be seen in Fig. 8. The film spontaneously breaks up into domains. This does not happen for the hydrogen covered film. The energy $\propto (AK_{\mathrm{eff}})^{1/2}$, ($K_{\mathrm{eff}}$ the effective anisotropy and A the exchange energy) to form a domain wall must be larger in this case compared to the uncovered Ni film of the same thickness. Assuming that it is K_{eff}, which is mostly affected by hydrogen exposure, we can conclude that indeed the anisotropy is enhanced by hydrogen exposure, so that the second spin reorientation transition is expected at larger thickness. A quantitative value, however cannot be derived from our data.

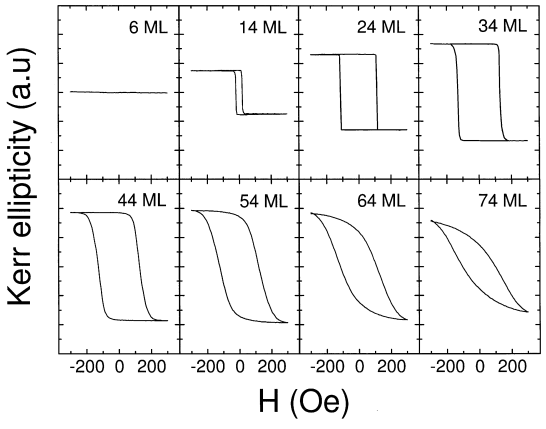

Fig. 8. Polar Kerr ellipticity hysteresis loops for different Ni film thickness, measured at 273 K. Note, an external applied magnetic field of 300 Oe is not enough to saturate the film magnetization of Ni films thicker than 50 ML.

5.3. Cu/Ni/Cu(0 0 1)

Separate determination of the surface ($K_{2\mathrm{s}}$) and interface anisotropy ($K_{2\mathrm{i}}$) is not possible in the experiments described above. Both anisotropies have the same thickness dependence and therefore only the sum of $K_{2\mathrm{s}}$ and $K_{2\mathrm{i}}$ can be calculated. However, separation can be achieved when the critical thickness observed for clean, H_2 covered and CO covered Ni films is compared to the critical thickness of a thin Ni film capped with Cu. In the latter case, the spin reorientation is influenced by $2K_{2\mathrm{i}}$ instead of $K_{2\mathrm{s}} + K_{2\mathrm{i}}$. Therefore, we have grown a Cu wedge perpendicular on a Ni wedge at 298 K. The Ni film was also grown at 298 K and not annealed prior the growth of the Cu wedge on top of it. Subsequently, Kerr microscopy images were taken at different substrate temperatures. In this manner, the change in spin reorientation transition as a function of Cu layer thickness and substrate temperature could be determined precisely.

Fig. 9 shows the critical thickness d_{c} as a function of sample temperature for the clean (squares) and the Cu covered (circles and triangles) Ni film (d_{c} was determined as the thickness where the remanent Kerr signal dropped to 10% of the extrapolated value). Growth of Cu on a Ni wedge also shifts the border of the spin reorientation transition to smaller film thickness. At a Cu coverage of one monolayer the critical thickness is reduced by 3 ML with respect to the clean Ni surface. Further growth of Cu does not change the spin reorientation transition any further. A shift to thinner Ni films upon Cu coverage was also observed by O'Brien et al. [11], however, the transition from in-plane to perpendicular magnetization shifted only by 1 ML from 7 to 6 ML in their measurements. The 6 ML of their Cu covered Ni film is close to our value considering the uncertainty in

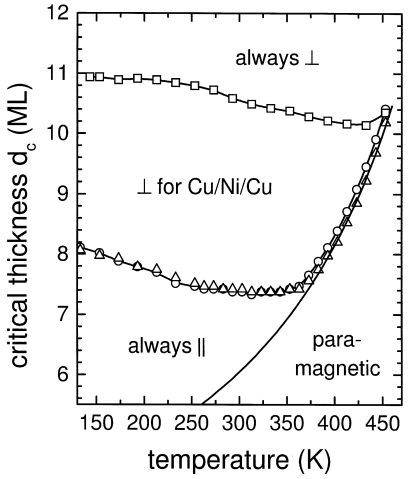

Fig. 9. Critical thickness of the spin reorientation transition of a Ni film versus sample temperature for the clean Ni surface (squares) and for the Ni surface capped with 2 ML Cu (triangles) and 5 ML Cu (circles). The solid line is a power law $T_C(d)/T_C(\infty) = 1 - (d/d_0)^{-\lambda}$ with $T_C(\infty)$ the bulk Curie temperature, $d_0 = 3.6$ ML and $\lambda = 1.2$.

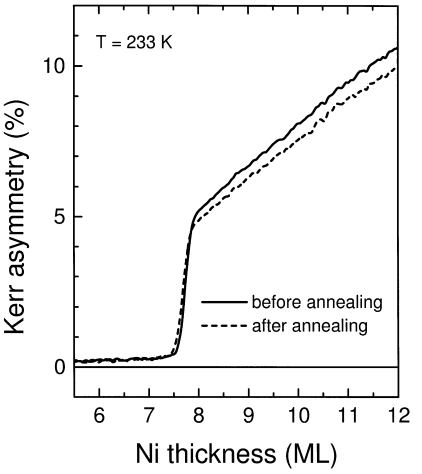

Fig. 10. Polar Kerr asymmetry versus Ni thickness at 233 K for a Ni wedge covered with 5 ML Cu. The solid (dashed) line represents the Kerr asymmetry before (after) annealing the film at 453 K.

the thickness determination of about 0.8 ML. The smaller shift we attribute to a partial hydrogen precoverage of the Ni film in their case. Our result, however, is completely inconsistent with the magnetoelastic model described by Bochi et al. [26], which predicts a shift of the reorientation transition towards higher thickness. The measurement of the critical thickness at different substrate temperatures is completely reversible. Annealing of the sandwich structure to 453 K for about 10 min does not influence the spin reorientation transition in the Ni film. This is illustrated in Fig. 10. This figure shows the Kerr asymmetry at 233 K, measured before and after annealing to 453 K. The solid line indicates the Kerr asymmetry measured on the Cu/Ni/Cu(0 0 1) sandwich directly after the preparation of the structure at 298 K, the dashed is the Kerr asymmetry after annealing to 453 K at the same temperature of 233 K as the first measurement. No change in the onset of the polar Kerr signal is observed (the small difference in the magnitude of the Kerr signal is within the experimental error). The shift of the data points towards higher values at about 350 K and above in Fig. 9 is not due to the increase of the thickness at which the magnetization switches from in-plane to perpendicular magnetization but is attributed to the transition from the ferromagnetic to the paramagnetic phase. The displayed data points above 350 K, therefore, do not indicate the film thickness at which the reorientation from perpendicular magnetization to in-plane magnetization occurs. They mark the boundary where the out-of-plane remanent magnetization disappears instead. The solid line in Fig. 9 is a power law $T_C(d)/T_C(\infty) = 1 - (d/d_0)^{-\lambda}$ with $T_C(\infty)$ the bulk Curie temperature, $d_0 = 3.6$ ML and $\lambda = 1.2$. Such a value of λ is commonly measured for many systems [48]. However, the values of $T_C(d)$ for a given thickness are lower by up to 60 K compared to those reported for the uncovered Ni film on Cu(0 0 1) [5,20]. Small differences in the thickness calibration partially may account for this. However, covering of the Ni film with a Cu cap layer also strongly reduces T_C [13]. In that experiment, a Cu coverage of 2.8 ML lowered T_C by more than 30 K.

5.4. Surface anisotropy energy

The interface and surface anisotropy of the uncovered, CO-, H_2- and Cu-covered Ni films can be calculated now from our measured critical

thicknesses as described in Section 2. In these calculations we took the value 30 μeV/atom for the strain induced volume anisotropy K_{2v} and for the shape anisotropy $2\pi M_s^2 = 7.5$ μeV/atom. In principle, there might be differences in the properties of the Cu/Ni and Ni/Cu interface. Our experimental observation that the spin reorientation transition is independent of the thickness of the Cu for thickness above 2 ML and thermally stable however, indicates that the two interfaces can be considered as equal. The interface anisotropy energy K_{2i} is then given by the expression $2K_{2i} = (2\pi M_s^2 - K_{2v}) \times d_c$. At 300 K we observed a critical thickness of $d_c = 7.4$ ML for the Ni film capped with Cu. This results in a value of $K_{2i} = -83$ μeV/atom for a single Cu/Ni interface.

The surface anisotropy K_{2s} for the clean Ni film at 300 K yields -153 μeV/atom, which follows from our measured critical thickness of 10.5 ML for the clean uncovered Ni film. This anisotropy energy $K_{2s} = -153$ μeV/atom at the Ni/vacuum interface is much larger than the anisotropy energy $K_{2i} = -83$ μeV/atom at the Ni/Cu interface. This is in agreement with a recent ab initio calculation by Uiberacker et al. [49] and with the experiment by O'Brien et al. [11]. The calculation shows that the band energy difference, and therefore the magnetic anisotropy energy, is much larger at the surface than at the interface. To compare with the result of theoretical calculations the values for K_{2s}, K_{2i}, K_{2v}, and $2\pi M_s^2$ have to be extrapolated to 0 K. The temperature dependence of $d_c(T)$ for the uncovered and the Cu covered Ni film is not very large as can be seen from Fig. 9. However, this is because the temperature dependence of K_{2i} and K_{2s} on the one hand and K_{2v} on the other hand are very similar. Because of the negative sign of K_{2i} and K_{2s} and the positive sign of K_{2v} the temperature dependence of $d_c(T)$ largely cancels. The temperature dependence of K_{2v}, however, is quite large and has been measured by Farle et al. [24]. If we take the extrapolated value $K_{2v} = 72$ μeV/atom at $T = 0$ K from Ref. [24] and our extrapolated critical thickness $d_c(0\text{ K}) = 11.6$ ML for the clean Ni surface we obtain $K_{2s} + K_{2i} \approx -700$ μeV/atom. This value is much larger than the result of two theoretical calculations which yield a value of about -100 μeV/atom [49,50]. However, in Ref. [49] the definitions of K_{2s} and K_{2i} are different from those used to analyze our experimental data. In the theoretical work K_{2s} and K_{2i} are essentially the magnetic anisotropy energy of the surface Ni layer and the interface Ni layer, respectively, while in the experimental work K_{2s} and K_{2i} are determined from the extrapolation down to zero film thickness. These two definitions lead to the same result only in the case that the magnetic anisotropy energy does not change with thickness in the interior of the film, which is, according to the calculation in Ref. [49], not fulfilled. A recent theoretical work by Henk et al. [51] indeed shows, that for Ni film thickness up to at least 10 ML the superposition of interface and surface part strongly deviates from the result of the calculation for the true thin film geometry, indicating, that the quantized thin film states significantly contribute to the magnetocrystalline anisotropy.

From the measurements of d_c of the adsorbate covered Ni films we can estimate the change in K_{2s} upon coverage of the surface with these adsorbates. If we take the measured critical thickness $d_c = 7.3$ ML for the CO covered Ni surface at 300 K, we obtain a surface anisotropy energy $K_{2s} = -81$ μeV/atom. Therefore, the absolute value of the surface anisotropy energy decreases dramatically upon CO adsorption. It seems that CO adsorption and Cu coverage re-establishes a more bulk like behavior of the surface. An even more drastic decrease in critical thickness is observed upon hydrogen adsorption. If we extrapolate the measured d_c of the H_2 covered Ni surface to 300 K we obtain $d_c = 6.8$ ML and $K_{2s} = -70$ μeV/atom. The measured critical thickness at 300 K as well as the calculated surface anisotropy energies are summarized in Table 1. From these measurements we can conclude that covering a Ni film with CO, H_2 and Cu reduces the surface anisotropy energy approximately by 50%. This reduction in surface anisotropy energy shifts the border of the spin reorientation transition to smaller Ni film thickness. The critical thickness is reduced by 4 and 3 ML upon H_2 and CO/Cu coverage, respectively.

The influence of hydrogen adsorption on the second spin reorientation transition can be discussed now too. The negative surface anisotropy

Table 1
Measured critical thickness d_c of the reorientation transition at $T = 300$ K and derived surface anisotropy energies K_{2s}. The surface anisotropy is derived using $K_{2v} = 30$ μeV/atom, and $2\pi M_s^2 = 7.5$ μeV/atom from Ref. [4]

	d_c (ML)	K_{2s} (μeV/atom)
Ni/Cu(0 0 1)	10.5	− 153
Cu/Ni/Cu(0 0 1)	7.4	− 83
CO/Ni/Cu(0 0 1)	7.3	− 81
H_2/Ni/Cu(0 0 1)	6.8	− 70

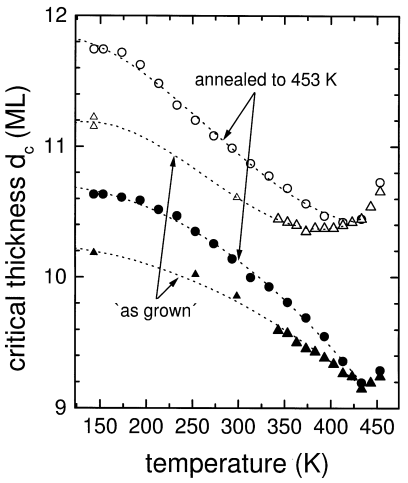

Fig. 11. Critical thickness of the spin reorientation transition of a Ni film versus sample temperature for a Ni wedge grown at 298 K (triangles) and the same wedge after annealing to 453 K (circles). Closed symbols: thickness at which the Kerr signal with 300 Oe external field dropped to 50% of the extrapolated polar Kerr signal. Open symbols: thickness at which the remanent Kerr signal dropped to 80% of the extrapolated polar Kerr signal.

energy causes in-plane magnetization. Hydrogen adsorption reduces this anisotropy, and therefore increases the thickness range in which out-plane magnetization is observed, i.e. the second spin reorientation transition shifts to thicker Ni film thickness. The measurement shown in Fig. 7 indeed indicate a shift in the second spin reorientation transition as discussed in detail in Section 5.2.

The influence of CO and especially H_2 adsorption on the magnetic properties of thin magnetic layers should even be considered in experimental setups with a good base pressure and without intentional gas exposure. For example, a hydrogen partial pressure of 3×10^{-11} mbar at 300 K will result in an equilibrium coverage of about 0.1 ML [43]. A decrease in temperature by 20 K or an increase of the hydrogen pressure by a factor of 10 will increase this coverage by more than a factor of 3 and this equilibrium coverage is already reached after 30 min. In our experiments (base pressure $< 4 \times 10^{-11}$ mbar) the possible effect of hydrogen adsorption is indicated by a small arrow in Fig. 6. In this measurement the amount of hydrogen adsorption was minimized by fast data acquisition during decreasing substrate temperature. Therefore, in general the effect of hydrogen adsorption on the spin reorientation transition can be more pronounced. Due to a higher desorption temperature, effects of CO adsorption on the magnetic properties are expected even at elevated sample temperatures. However, because of the usually much smaller partial pressure of CO compared to H_2 unintentional CO adsorption can be avoided much easier than H_2 adsorption.

5.5. Influence of surface roughness

For the above measurements the Ni film was annealed to 453 K for several minutes which resulted in smooth films [23] but did not change the magnetic properties besides a small reduction in the coercive field [46]. It has been shown that surface roughness may affect d_c as well [14,52]. We therefore compared the critical thickness obtained from the annealed film with the d_c derived from measurements taken directly after the growth of the Ni wedge at 298 K. This comparison is shown in Fig. 11 with circles for the annealed and triangles for the unannealed Ni film. The open symbols represent the critical thickness determined from the vanishing of the *remanent* polar Kerr signal (drop to 80% of the extrapolated Kerr signal as illustrated in the inset of Fig. 4), while the solid symbols represent the critical thickness determined from the Kerr signal with an applied magnetic field of 300 Oe (drop to 50% of the Kerr signal). The data for the unannealed film were first collected by lowering the temperature, starting from 300 K directly after the growth of the Ni film. As discussed

above, the critical thickness at the lowest temperature might be already reduced slightly due to hydrogen adsorption. The data above room temperature were taken afterwards with increasing temperature. Above 320 K the hydrogen, adsorbed during the growth of the Ni film and during the time the sample was below room temperature, is completely desorbed. Therefore, the open triangles above 320 K indicate the vanishing of the remanent polar magnetization of the clean film with the 'as-grown' surface morphology. At high temperatures close to the Curie temperature the remanent polar Kerr signal disappears below a thickness of 10 ML. This might be caused by the formation of domains [53] with domain sizes below the resolution of our Kerr microscope [45]. The influence of domain formation is absent in the critical thickness derived from the Kerr signal with applied field (solid symbols). In both cases, a reduced critical thickness of up to about 0.4 ML is found for the 'as-grown' (rougher) Ni wedge compared to the annealed film. At elevated temperatures smoothing of the 'as-grown' film becomes significant and the datapoints of the 'as-grown' film merges into those of the annealed film.

Bruno has explained this reduction within a simple phenomenological model by a roughness induced decrease of the effective surface anisotropy (ΔK_{2s}) [52,54]. Two separate contributions to this decrease can be distinguished. First, step edge atoms contribute only half of the surface anisotropy of atoms in the terrace. Therefore, $\Delta K_{2s} = R_{\text{step/terrace}} \times K_{2s}/2$, with $R_{\text{step/terrace}}$ the ratio between the number of step edge atoms and the number of atoms in the terrace. Secondly, the shape anisotropy decreases with surface roughness. Following Ref. [52], this contribution can be calculated from the terrace average width ξ and height 2σ. Shen et al. [46] derived from STM images a rms roughness of 1.5 Å for a 10 ML thick film. The average island distance is about 60 Å. Using these parameters and the theory of Ref. [52] we find that the change of the shape anisotropy is less than 1 μeV/atom and can be ignored completely in the present case. The total contribution of the roughness to the surface anisotropy ΔK_{2s} is calculated to $+15$ μeV/atom. As it is evident from Fig. 9 of Ref. [46] annealing of the 10.2 ML Ni film results in strong reduction of roughness. σ is reduced by approximately a factor of 2 and the average island distance is increased by a factor of 2. The remaining contribution of the roughness to the surface anisotropy of this annealed 10.2 ML Ni film is only $+4$ μeV/atom. For these parameters a reduction of the critical thickness of 0.5 ML is calculated, close to our experimentally observed change of less than 0.4 ML. This shift in spin reorientation transition is small compared to the observed shift after CO- and H_2-adsorption or Cu growth. We therefore conclude that changes in the surface morphology have only a minor effect on d_c.

6. Summary

We observed a strong reduction in the critical thickness of the spin reorientation transition in Ni/Cu(0 0 1) when covered with CO, H_2, or Cu cap layers. The reduction in critical thickness after CO and H_2 adsorption is about 3 and 4 ML, respectively. The shift in the spin reorientation transition to smaller Ni film thickness is attributed to a decrease in the negative surface anisotropy energy. Calculation of this surface anisotropy for CO, H_2 and Cu covered Ni films yield values about 50% smaller than for uncovered Ni films. Compared to CO and H_2 adsorption, the influence of surface roughness is negligible. A shift of less than 0.4 ML is observed after annealing a room temperature grown Ni film at $T = 453$ K. The observed influence of CO and H_2 on the magnetic properties in Ni/Cu(0 0 1) may well be representative for the influence of adsorbates on thin films in general.

Acknowledgements

We thank U. Gradmann for stimulating discussions.

References

[1] C. Liu, S.D. Bader, J. Vac. Sci. Technol. A 8 (1990) 2727.
[2] Z.Q. Qiu, J. Pearson, S.D. Bader, Phys. Rev. Lett. 70 (1993) 1006.

[3] H.P. Oepen, M. Speckmann, Y. Millev, J. Kirschner, Phys. Rev. B 55 (1997) 2752.
[4] B. Schulz, K. Baberschke, Phys. Rev. B 50 (1994) 13467.
[5] F. Huang, M.T. Kief, G.J. Mankey, R.F. Willis, Phys. Rev. B 49 (1994) 3962.
[6] W.L. O'Brien, B.P. Tonner, J. Appl. Phys. 79 (1996) 5623.
[7] S.Z. Wu, G.J. Mankey, F. Huang, R.F. Willis, J. Appl. Phys. 76 (1994) 6434.
[8] W.L. O'Brien, B.P. Tonner, Phys. Rev. B 49 (1994) 15370.
[9] C. Chang, J. Appl. Phys. 68 (1990) 4873.
[10] R. Jungblut, M.T. Johnson, J. aan de Stegge, A. Reinders, F.J.A. den Broeder, J. Appl. Phys. 75 (1994) 6424.
[11] W.L. O'Brien, T. Droubay, B.P. Tonner, Phys. Rev. B 54 (1996) 9297.
[12] G. Bochi, C.A. Ballentine, H.E. Inglesfield, C.V. Thompson, R.C. O'Handley, Phys. Rev. B 53 (1996) R1729.
[13] P. Srivastava, F. Wilhelm, A. Ney, M. Farle, H. Wende, N. Haack, G. Ceballos, K. Baberschke, Phys. Rev. B 58 (1998) 5701.
[14] M. Zheng, J. Shen, P. Ohresser, C.V. Mohan, M. Klaua, J. Barthel, J. Kirschner, J. Appl. Phys. 85 (1999) 5060.
[15] H.J. Elmers, U. Gradmann, J. Appl. Phys. 63 (1988) 3664.
[16] W. Göpel, Surf. Sci. 85 (1979) 400.
[17] M. Weinert, J.W. Davenport, Phys. Rev. Lett. 54 (1985) 1547.
[18] G.J. Mankey, M.T. Kief, F. Huang, R.F. Willis, J. Vac. Sci. Technol. A 11 (1993) 2034.
[19] K. Baberschke, Appl. Phys. A 62 (1996) 417.
[20] M. Farle, Rep. Prog. Phys. 61 (1998) 755.
[21] M.T. Johnson, P.J. Bloemen, F.J.A. den Broeder, J.J. de Vries, Rep. Prog. Phys. 59 (1996) 1409.
[22] M. Farle, W. Platow, A.N. Anisimov, P. Poulopoulos, K. Baberschke, Phys. Rev. B 56 (1997) 5100.
[23] J. Shen, M.-T. Lin, J. Giergel, C. Schmidthals, M. Zharnikov, C.M. Schneider, J. Kirschner, J. Magn. Magn. Mater. 156 (1996) 104.
[24] M. Farle, B. Mirwald-Schulz, A.N. Anisimov, W. Platow, B. Baberschke, Phys. Rev. B 55 (1997) 3708.
[25] S. Müller, B. Schulz, G. Koska, M. Farle, K. Heinz, K. Baberschke, Surf. Sci. 364 (1996) 235.
[26] G. Bochi, C.A. Ballentine, H.E. Inglefield, C.V. Thompson, R.C. O'Handley, H.J. Hug, B. Stiefel, A. Moser, H.-J. Güntherodt, Phys. Rev. B 52 (1995) 7311.
[27] S. Andersson, Solid State Commun. 21 (1977) 75.
[28] J.C. Bertolini, B. Tardy, Surf. Sci. 102 (1981) 131.
[29] R.G. Tobin, S. Chiang, P.A. Thiel, P.L. Richards, Surf. Sci. 140 (1984) 393.
[30] R. Klauser, W. Spiess, A.M. Bradshaw, B.E. Hayden, J. Electron. Spectosc. Relat. Phenom. 38 (1986) 187.
[31] P. Uvdal, P.-A. Karlsson, C. Nyberg, S. Andersson, N.V. Richardson, Surf. Sci. 202 (1988) 167.
[32] J. Lauterbach, M. Wittmann, J. Küppers, Surf. Sci. 279 (1992) 287.
[33] M. Passler, A. Ignatiev, F. Jona, D.W. Jepsen, P.M. Marcus, Phys. Rev. Lett. 43 (1979) 360.
[34] S. Andersson, J.B. Pendry, Phys. Rev. Lett. 43 (1979) 363.
[35] M. Onchi, H.E. Farnsworth, Surf. Sci. 11 (1968) 203.
[36] J.C. Tracy, J. Chem. Phys. 56 (1972) 2736.
[37] J.P. Biberian, M.A. van Hove, Surf. Sci. 118 (1982) 443.
[38] M. Kiskinova, D.W. Goodman, Surf. Sci. 108 (1981) 64.
[39] D.W. Goodman, J.T. Yates Jr., T.E. Madey, Surf. Sci. 93 (1980) L135.
[40] S. Andersson, Chem. Phys. Lett. 55 (1978) 185.
[41] I. Stensgaard, F. Jakobsen, Phys. Rev. Lett. 54 (1985) 711.
[42] K. Christmann, G. Ertl, O. Schober, Surf. Sci. 40 (1973) 61.
[43] K. Christmann, O. Schober, G. Ertl, M. Neumann, J. Chem. Phys. 60 (1974) 4528.
[44] J. Lapujoulade, K.S. Neil, Surf. Sci. 35 (1973) 288.
[45] J. Giergiel, J. Kirschner, Rev. Sci. Instr. 67 (1996) 2937.
[46] J. Shen, J. Giergiel, J. Kirschner, Phys. Rev. B 52 (1995) 8454.
[47] R. Vollmer, Th. Gutjahr-Löser, J. Kirschner, S. van Dijken, B. Poelsema, Phys. Rev. B 60 (1999) 6277.
[48] U. Gradmann, in: K.H.J. Buschow (Ed.), Handbook of Magnetic Materials, Vol. 7, Elsevier, Amsterdam, 1993.
[49] C. Uiberacker, J. Zabloudil, P. Weinberger, L. Szunyogh, C. Sommers, Phys. Rev. Lett. 82 (1999) 1289.
[50] A. Lessard, T.H. Moos, W. Hübner, Phys. Rev. B 56 (1997) 2594.
[51] J. Henk, A.M.N. Niklasson, B. Johansson, Phys. Rev. B 59 (1999) 9332.
[52] P. Bruno, J. Appl. Phys. 64 (1988) 3153.
[53] P. Poulopoulos, M. Farle, U. Bovensiepen, K. Baberschke, Phys. Rev. B 55 (1997) R11961.
[54] P. Bruno, J. Phys. F 18 (1988) 1291.